The wear and rolling contact fatigue behaviour of AAR Class C wheel and R350 HT rail using a twin-disc tribometer under dry conditions

Bridget Sikhondze[1*], *Charles* Siyasiya[1], *Roelof* Mostert[1] and *Joseph* Moema[2]

[1]Metallurgical Engineering, Department of Materials Science and Engineering, University of Pretoria, Pretoria, South Africa
[2] Advanced Materials Division, MINTEK, Randburg, South Africa

Abstract. The wear and rolling contact fatigue (RCF) behaviour of AAR Class C wheels and R350 HT rail was investigated under dry testing conditions. The RCF crack morphology, length and depth were of particular interest and, therefore were investigated using the twin-disc tribometer by varying the number cycles from 20,000 to 120,000. Thereafter, the wear behaviour and surface/subsurface degradation were characterised. It was found that AAR Class C wheel failed mainly through wear damage, whilst R350 HT rail showed more wear resistance but poorer RCF life.

1 Introduction

Wear and rolling contact fatigue are two types of damage experienced by the rail/wheel system. Wear refers to the gradual removal of material from contacting surfaces due to an applied load and can occur under dry or wet conditions. The mechanisms by which wear occurs have been categorised by way of wear maps, where it is classed as either mild, severe or catastrophic[1], [2]. In contrast, rolling contact fatigue (RCF) is the degradation of rail and wheel material due to the repeated application of force and contact pressures.

The contact area between rail and wheel in the rail/ wheel system is extremely small, but experiences high loading. With repeated application of load, shear deformation occurs beneath the surface. Once the ductility limit is reached, cracks initiate and grow, eventually resulting in the removal of material. This process is known as ratcheting [3]. An increase in contact pressure and traffic volume on railways can accelerate wear, significantly reducing the service life of the rail/wheel system.[4], [5] . In recent years, however, RCF has been identified as the predominant mode of damage, contributing to safety incidents and increasing maintenance and replacement costs[6]. The relationship between wear and RCF is competitive in nature; reducing the wear rate promotes the formation of RCF cracks, whilst enhancing the resistance to RCF increases the wear rate[7] Understanding this relationship is vital for developing effective repair and maintenance models for rail and wheel steels. The microstructures of rail and wheel steels influence their wear and RCF performance. Rail wheel steels with a lower volume fraction of ferrite have better wear performance and

toughness, whereas fully pearlitic rails with fine interlamellar spacing possess a good combination of wear and RCF resistance [8], [9].

Numerous studies have investigated the effect of contact pressure and slip ratio on the wear and rolling contact behaviour. These studies have shown that the wear rate increases with increasing contact stress whilst an increase in the slip ratio enhances crack propagation [7]. Despite many studies having focused on the impact of slip ratio and contact pressures on wear and RCF behaviour [6], [10], [11], few have considered solely, the influence of the number of cycles. In the context of heavy-haul rail operations in South Africa, the pairing of Association of American Railroads (AAR) Class C wheels with R350 HT rails is of particular relevance. It is essential, therefore, that the wear and RCF behaviour of these rail steels be studied in depth. Specifically, understanding crack length, crack depth, and propagation is vital for informing maintenance and repair schedules. In real-world railway operations, maintenance schedules are often guided by a distance-based threshold. For instance, inspections and repairs are scheduled after 1 million cycles or 160000 km of service in South Africa [12]. Incorporating such distance-based metrics into lab-based fatigue or wear studies can help bridge the gap between experimental findings and practical applications. The aim of this study was to investigate the influence of number of cycles on the wear and RCF behaviour of AAR Class C wheel run against R350 HT rail under dry contact conditions.

2 Experimental method

2.1 Test specimens

Test specimens of R350 HT rail and AAR Class C wheel were sectioned from the rail head and wheel tread, respectively. The dimensions of these specimens were set to a 30 mm inner diameter, 50 mm outer diameter and 5 mm thickness. Table 1 shows the chemical composition of R350 HT rail and AAR Class C wheel obtained using spark emission spectroscopy. The table also shows the interlamellar spacing and hardness values of these rail and wheel steels. The interlamellar spacing was calculated using the linear intercept method whereby a line of known length was drawn at right angles to the cementite lamellae in each pearlite colony. The length of the line was subsequently divided by the amount of intersections to determine the spacing. This process was replicated on five separate colonies and an average spacing calculated.

Table 1. Chemical compositions, interlamellar spacing and initial hardness values of AAR Class C wheel and R350 HT rail.

Chemical composition (wt%)	C	Mn	Cr	Ni	Si	F	S	N	Interlamellar Spacing (nm)	Hardness HV10
R350 HT Rail	0.79	1.17	0.197	0.061	0.388	0.013	0.038	0.019	99 ± 7.4	398 ± 7.4
AAR Class C Wheel	0.70	0.87	0.168	-	0.353	0.017	0.0060	-	140 ± 14.9	340 ± 14.9

The as-received microstructures of AAR Class C wheels and R350 HT rails are shown in Fig. ***1*** below. These micrographs were obtained using a scanning electron microscope (SEM), after the samples were ground and polished to a 1 µm finish, then etched with 2% Nital solution.

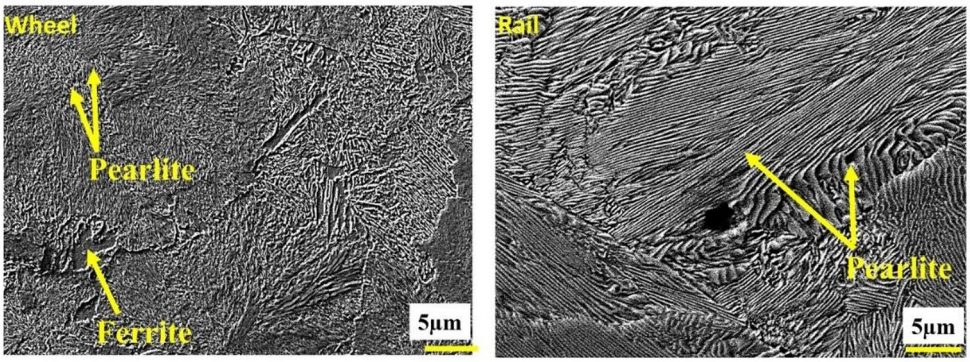

Fig. 1. As-received micrographs of AAR Class C wheel and R350 HT rail.

2.2 Test procedure

Rolling-sliding wear tests were conducted at room temperature, ambient relative humidity and under dry conditions. A rolling-sliding wear test is defined as one complete rotation of the rail roller material, with a slip ratio greater than 0%. Pure rolling conditions are experienced at 0% slip whilst 100% slip corresponds to pure sliding. For these tests, a manually operated twin-disc tribometer designed and built at the University of Pretoria was used in this study (Fig. ***2)***.

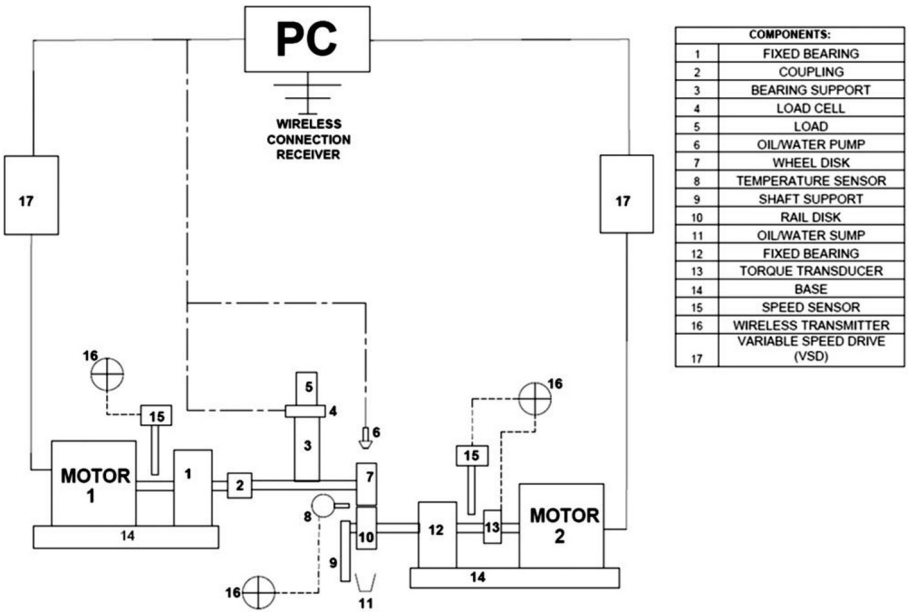

Fig. 2. A schematic of the twin disc tribometer used for wear and RCF tests at the University of Pretoria.

The rig was configured such that the two discs ran against each other at opposite angular speeds under a specified applied load. The shafts onto which the specimens were mounted, were connected to separate motors which were independently controlled. In the setup, the wheel acted as the braking disc while the rail functioned as the driving disk. Tachometers equipped with a digital display, together with a magnet placed on each shaft as a sensor, ensured that the correct speeds, and therefore, slip was measured during the duration of

testing. A 2-ton scissor jack was used to apply the required load at the contact, and the load itself was measured using a 10kN C9C load cell. The applied load was captured using a QuantumX (MX440B) data acquisition system connected to a personal computer (PC) and interpreted by Catman software. For these experiments, a load of 1.8kN and speeds of 340 rpm for the AAR Class C wheel, and 320 rpm for the R350 HT rail were used. This gave a slip of 6% and it was calculated as follows:

$$Slip\ (\%) = \frac{(R_1 \times N_1) - (R_2 \times N_2)}{(R_1 \times N_1) + (R_2 \times N_2)} \quad [5]$$

Where R_1 and R_2 are the disc radii of the wheel and rail, respectively, and N_1 and N_2 are their angular velocities. The load of 1.8kN corresponds to a Hertzian contact stress of 1.04GPa which is representative of typical in-service rail-wheel contact stresses. Whilst the load and slip were kept constant, the number of cycles was varied. Tests were conducted at 20000, 30000, 40000, 80000 and 120000 cycles, which equate to rolling distances of 3.14 km, 4.71 km, 6.28 km, 12.57 km and 18.86 km, respectively. To obtain statistically significant results, each test was repeated three times for each cycle.

Prior to testing, samples of rail and wheel disc were cleaned in ethanol using an ultra-sonic bath. Thereafter, they were weighed using a mass balance with an accuracy of 0.1 mg. After each test, samples were again cleaned with ethanol in an ultrasonic bath, and mass losses were measured using the same balance. The wheel and rail samples were then sectioned, after which they were ground, polished and etched. Optical microscopy (OM) and scanning microscopy (SEM) were employed to analyse the deformed layer and to observe surface and subsurface cracks. ImageJ software was used to measure the crack length and depth.

3 Results and discussion

3.1 Wear rates and mass losses

The mass losses of both AAR Class C wheels and R350 HT rails are shown in Fig. ***3***. It can be observed that the amount of material lost from the wheel and rail was almost identical after the first 20000 cycles. This result is on trend with findings by other researchers, using different pairings of pearlitic rail and wheel material [3], [8]. The initial similarity in mass loss can be ascribed to early-stage contact mechanics, where asperity-level interactions dominate. During this phase, surface roughness and waviness are gradually reduced through micro-polishing, leading to the establishment of a more stable contact interface [5]. Following this, after 40000 cycles, the mass loss and wear rate (Fig. ***4***) increased for the wheel. The high wear rate observed for the wheel after 40000 cycles was due to the formation of white etching layer (WEL), a nano crystalline, heavily dislocated surface with a high crack density [3], [5]. Being brittle, its presence contributes to the mass loss of the wheel and drives up the wear rate. Throughout the test cycles, the wheel consistently exhibited higher mass loss compared to the rail. These results can be linked to the differing microstructures which give rise to the different mechanical properties of the two materials. The R350 HT rail, being fully pearlitic and possessing a finer lamellar spacing (99 nm), is the harder material (398 ± 7.4 HV10) and therefore has greater wear resistance. However, the AAR Class C wheel which contains proeutectoid ferrite and a coarse interlamellar spacing (approximately 140 nm), is relatively softer (340 ± 14.9 HV10) and more susceptible to wear. This observation is in line with existing literature, which states that when similar alloys are in contact, the harder material is the more wear resistant. Similar wear rate values were displayed again by

both the AAR Class C wheel and R350 HT rail after 80000 cycles, and thereafter the wear rate began to decrease.

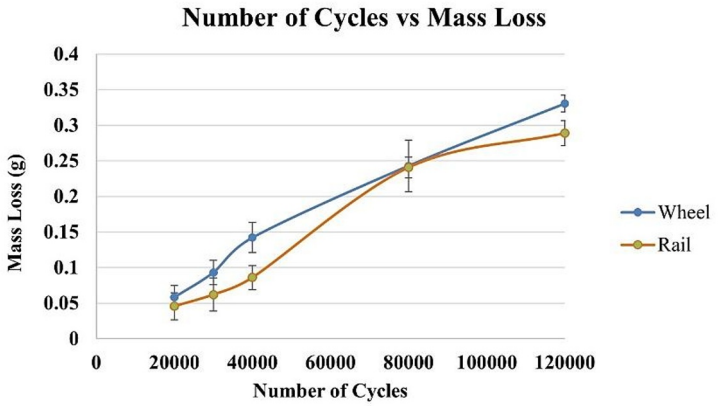

Fig. 3. Number of cycles versus mass losses of AAR Class C wheels and R350 HT rail.

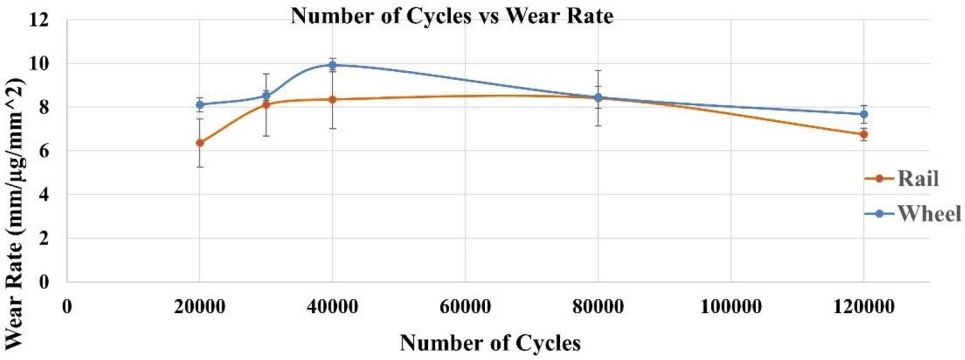

Fig. 4. Number of cycles versus wear rate of AAR Class C wheel and R350 HT rail.

3.2 Fatigue cracks, depth of deformation and crack depth

The evolution in crack morphology in wheel and rail material after 20000 and 80000 cycles is observed in Fig. ***6***. After 20000 cycles the cracks in both the wheel and rail were surface cracks but their physical characteristics differed notably. In the wheel, the cracks after this cycle were discontinuous and propagated either downwards or ran parallel to the rolling direction. Contrastingly, those in the rail were continuous and were only oriented parallel to the rolling direction. These differences can be attributed to the microstructures of the respective materials. In the ferritic-pearlitic wheel, cracks propagated along the soft ferrite [7] and the coarse lamellar colonies provided little resistance to crack propagation, which enabled the cracks to change direction easily [5] . In the case of the fully pearlitic rail, the fully pearlitic rail material guided crack propagation more uniformly through the pearlite colonies. After 80000 cycles, the cracks in the rail displayed more complex features; they were multi layered, with crack branching and interlocking also occurring. In contrast, after the same number of cycles, the white etching layer (WEL) discussed in Section 3.1, prevailed

in the wheel roller, and was responsible for high wear rate depicted Fig. ***4***. This layer has been reported in other studies involving different rail and wheel pairings [5], [11]

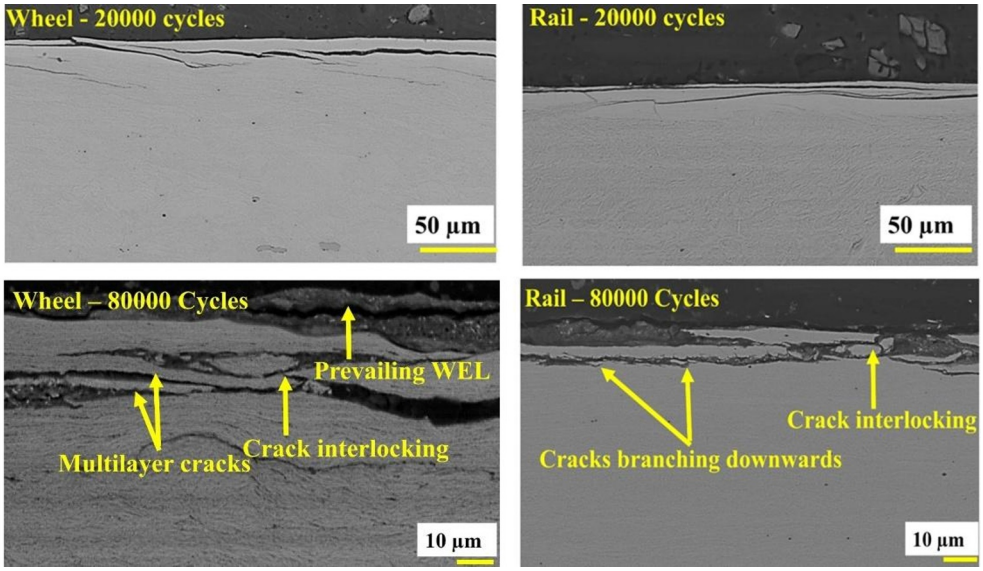

Fig. 5. Crack morphologies of R350 HT rail and AAR Class C wheel after 20000 and 80000 cycles.

Presented in Table 2 are crack length and crack depth values. Crack length and depth values were higher in the rail than those of the wheel with each cycle. Specifically, crack lengths were 49% higher after 20000 cycles, 44% higher after 80000 cycles and 18% higher after 120000 cycles. These results are consistent with the wear trends shown in Fig. ***4***, where the AAR Class C wheel exhibited a higher wear rate. This indicates that in the wheel, material is predominantly removed through wear, thereby reducing crack propagation, while the rail experiences less wear but more extensive crack growth. The greater crack depth observed in the rail corresponds to a deeper deformation zone, as depicted by Fig. ***6***. The wheel's microstructure, which includes proeutectoid ferrite, undergoes strain hardening more rapidly [5], [7], [13] . However, this means that the ductility limit is reached just as quickly, promoting crack initiation. The softer nature of the wheel material results in higher wear rate and thus a shallower deformation depth. Conversely, the rail's fully pearlitic microstructure enhances hardness, reducing wear and allowing for a deeper deformation layer.

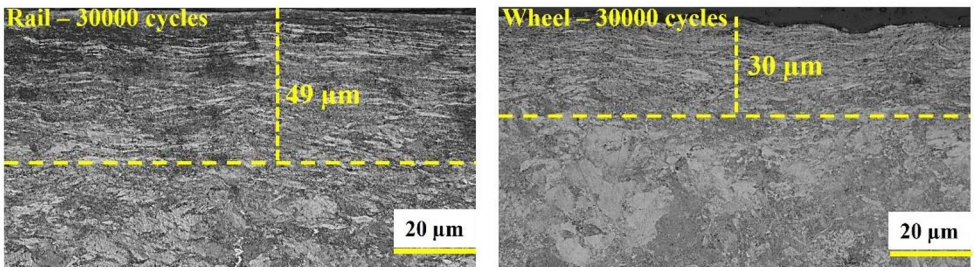

Fig. 6. OM micrographs showing plastically deformed region in AAR Class C wheel and R350 HT rail after 30000 cycles.

Table 2. Average crack length and crack depth values of AAR Class C wheel and R350 HT rail.

Material	**R350 HT Rail**		**AAR Class C Wheel**	
Number of cycles	Crack length (µm)	Crack Depth (µm)	Crack length (µm)	Crack Depth (µm)
30000	53 ± 8	34 ± 13	27 ± 2	30 ± 7
80000	62 ± 4	32 ± 12	41 ± 3	30 ± 11
120000	98 ± 3	27 ± 5	80 ± 4	**22 ± 1**

4 Conclusions

The wear and rolling contact fatigue (RCF) behaviour of AAR Class C wheels and R350 HT rails was investigated using a twin-disc tribometer under dry contact conditions. Based on the experimental results, the following conclusions were reached:

- The wear and RCF performance of the AAR Class C wheel and R350 HT rail is not only influenced by contact conditions such as slip and load but also by the number of loading cycles. As the number of cycles increased, surface damage evolved progressive from mild wear to severe RCF, culminating in catastrophic failure after 120,000 cycles.

- The softer AAR Class C wheel material experienced damage primarily through wear, with limited crack propagation. In contrast, the harder R350HT rail material showed greater resistance to wear but was more susceptible to RCF crack initiation and growth, indicating a trade-off between wear resistance and rolling contact fatigue resistance.

References

[1] R. Lewis and U. Olofsson, Mapping rail wear regimes and transitions. J.Wear. **257**, 721–729, (2004). https://doi.org/10.1016/j.wear.2004.03.019

[2] W. J. Wang, S. R. Lewis, R. Lewis, A. Beagles, C. G. He, and Q. Y. Liu, The role of slip ratio in rolling contact fatigue of rail materials under wet conditions. J.Wear. **376–377**, 1892–1900, (2017). https://doi.org/10.1016/j.wear.2016.12.049

[3] R. S. Miranda, A. B. Rezende, S. T. Fonseca, F. M. Fernandes, A. Sinatora, and P. R. Mei, Fatigue and wear behavior of pearlitic and bainitic microstructures with the same chemical composition and hardness using twin-disc tests. J.Wear. **494–495**, (2022). https://doi.org/10.1016/j.wear.2022.204253

[4] T. P. Leso, C. W. Siyasiya, R. J. Mostert, and J. Moema, Study of rolling contact fatigue, rolling and sliding wear of class B wheel steels against R350HT and R260

rail steels under dry contact conditions using the twin disc setup. J. Triboint. **174**, (2022). https://doi.org/10.1016/j.triboint.2022.107711

[5] R. S. Miranda, A. B. Rezende, A. C. Carvalho, S. T. Fonseca, A. Sinatora, and P. R. Mei, The role of microstructure on the wear and rolling contact fatigue of railway steels. J.Wear. **548–549**, (2024). https://doi.org/10.1016/j.wear.2024.205398

[6] Y. Hu, L.Zhou, H.H. Ding, G.X. Tan, R. Lewis, Q.Y. Liu, J. Guo, W.J. Wang, Investigation on wear and rolling contact fatigue of wheel-rail materials under various wheel/rail hardness ratio and creepage conditions. J.Triboint. **143**, (2020). https://doi.org/10.1016/j.triboint.2019.106091

[7] N. Tosangthum, R.Krataitong, P.Wila, H.Koipraset, H. Buncham, P.Kansuwam, A. Manonukul and P.Sheppard, Dry rolling-sliding wear behavior of ER9 wheel and R260 rail couple under different operating conditions. J.Wear. **518–519**, (2023). https://doi.org/10.1016/j.wear.2023.204636

[8] S. M. Hasan, D. Chakrabarti, and S. B. Singh, Dry rolling/sliding wear behaviour of pearlitic rail and newly developed carbide-free bainitic rail steels. J.Wear. **408–409**, 151–159, (2018). https://doi.org/10.1016/j.wear.2018.05.006

[9] A. Kapito, "The Design of a Carbide-Free Alloy Composition and Heat Treatment Process for Forged Rail Wheel Application in South Africa", Ph.D. Dissertation, University of Pretoria, Faculty of Engineering, the Built Environment and Information Technology (2019).

[10] Y. Hu, L.C. Guo, M. Maiorino, H.H. Ding, R. Lewis, E. Meli, A. Rindi, Q.Y. Liu, and W.J. Wang, Dry rolling/sliding wear behaviour of pearlitic rail and newly developed carbide-free bainitic rail steels. J.Wear. **460–461**, (2020). https://doi.org/10.1016/j.wear.2020.203455

[11] Y. Fan, X. Gui, M. Liu, X. Wang, B. Bai, and G. Gao, Comparison of wear and rolling contact fatigue behaviours of bainitic and pearlitic rails under various rolling-sliding conditions. J.Wear. **508–509**, (2022). https://doi.org/10.1016/j.wear.2022.204474

[12] Global Railway Review, globalrailwayreview.com/news/114962//bombadier-traxxx-locomotives-southafrica/ (accessed 7/9/2025).

[13] Z. Y. Han, H.H. Wang, W. J., Wang, S.Y. Zhang, D.M. Lin, Y.Wang, H.h.Ding, Z.R. Zhou, and Q.Y. Liu, The correlation between material deformed microstructure and rolling contact fatigue crack propagation of U71Mn rail when matching with CL60 wheel, J.Triboint., **200**,2024). https://doi.org/10.1016/j.triboint.2024.110069

.